MODELING THE CYCLIC UNDRAINED BEHAVIOR OF SAND WITH INITIAL STATIC SHEAR STRESS

Gabriele CHIARO[1], Junichi KOSEKI[2] and L.I.N. DE SILVA[3]

ABSTRACT: This paper proposes a cyclic elasto-plastic model for simulating the undrained behavior of saturated sand with initial static shear (i.e., sloped ground) subjected to cyclic loading (i.e., earthquake). The model can describe both monotonic and cyclic torsional shear behaviors of saturated sand under drained and/or undrained conditions; moreover, it is capable of simulating qualitatively the stress-strain relationship and the effective stress path, even after the specimen achieves fully liquefied state. Its effectiveness is verified by simulating the results of undrained cyclic torsional shear tests on loose Toyoura sand specimens with initial static shear stress under stress-reversal and non-reversal loading conditions.

Key Words: elasto-plastic model, cyclic loads, initial static shear, sand, stress-dilatancy behavior, stress-strain relationship

INTRODUCTION

In the last decades, due mainly to the expansion of residential and industrial sites in areas highly vulnerable to liquefaction, such as coastal and river areas, there has been the need to develop efficient and economic countermeasures against liquefaction in order to decrease seismic damage to buildings, infrastructures and lifeline facilities as well as natural and man-made slopes. In order to satisfy such needs, it is definitely required to incorporate a more elaborate constitutive model into numerical codes (e.g., FEM, DEM, etc) which can describe the liquefaction behavior of sand during cyclic loading (i.e., earthquakes). This study would contribute to improve the understanding of the complicated static shear stress effects on cyclic behavior of sand.

This paper puts forward a cyclic elasto-plastic model which makes it possible to simulate the effects of initial static shear (i.e., slope ground conditions) on the undrained cyclic behavior of saturated sand, which leads to liquefaction-induced failure of natural and artificial slopes and consequent large shear strain development, as shown during past earthquakes events (e.g., 1964 Great Alaskian, USA; 1964 Niigata & 1983 Nihon-kai Chubu, Japan; etc).

The proposed model is an improvement over the prior model developed by De Silva (2008) at the Institute of Industrial Science (IIS), University of Tokyo, for the reason that initial static shear stress component, representative of sloped ground conditions, is introduced in this model by simulating a monotonic drained shear loading path before the undrained one. Therefore, a two-phase (drained followed by undrained) monotonic loading behavior, described in terms of both stress-strain

[1] Associate Research Fellow, University of Wollongong, Australia (Former PhD Student & Postdoctoral Fellow, University of Tokyo)
[2] Professor, Institute of Industrial Science, University of Tokyo
[3] Senior Lecturer, University of Moratuwa, Sri Lanka (Former PhD Student & Postdoctoral Fellow, University of Tokyo)

relationship and effective stress path, is generated by means of initial static shear conditions. Features of subsequent cyclic stress-strain relationship are kept as those employed previously by De Silva (2008). On the other hand, to describe the generation of pore water pressure during the undrained cyclic loading, an anisotropic over-consolidation boundary surface (AOC) is proposed; it takes into consideration the combined effects of over-consolidation and initial static shear stress. The AOC features are introduced into the empirical four-phase stress-dilatancy relationship formulated by De Silva (2008).

Applicability of the proposed model is verified by simulating the experimental results that were conducted by Chiaro et al. (2011a, b) in order to study the effect of initial static shear stress on the undrained cyclic behavior of saturated Toyoura sand.

MODELING THE CYCLIC STRESS-STRAIN BEHAVIOR OF SAND WITH STATIC SHEAR

Modeling the two-phase skeleton curve using GHE model

Monotonic stress-strain relationship (i.e., skeleton curve) of sand subjected to torsional shear loading can be modeled by using the well known Generalized Hyperbolic Equation (GHE; Tatsuoka and Shibuya, 1992), as described by Eq. (1):

$$Y = \frac{X}{\dfrac{1}{C_1(X)} + \dfrac{X}{C_2(X)}} \tag{1}$$

where, X and Y are the normalized plastic shear strain and the shear stress parameters, respectively. $C_1(X)$ and $C_2(X)$ are function of strain:

$$C_1(X) = \frac{C_1(0)+C_1(\infty)}{2} + \frac{C_1(0)-C_1(\infty)}{2}\cos\left\{\pi \Big/ \left(\left|\frac{\alpha'}{X}\right|^{m_t} + 1\right)\right\} \tag{2}$$

$$C_2(X) = \frac{C_2(0)+C_2(\infty)}{2} + \frac{C_2(0)-C_2(\infty)}{2}\cos\left\{\pi \Big/ \left(\left|\frac{\beta'}{X}\right|^{n_t} + 1\right)\right\} \tag{3}$$

All the coefficients in Eqs. (2) and (3) can be determined by fitting the experimental data plotted in terms of Y/X vs. X relationship, as shown in the example in Fig. 1. Note that, $C_1(X=0)$ is the initial plastic shear modulus, while $C_2(X=\infty)$ represents the normalized peak strength of the material.

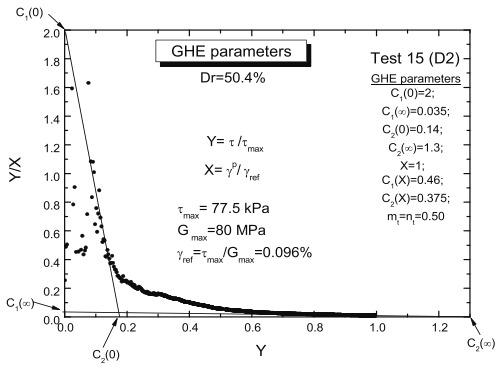

Figure 1 Evaluation of GHE parameters for a drained monotonic torsional shear test

In this paper, for both drained and undrained conditions, X and Y are defined as follows:

$$X = \gamma^{p} / \gamma^{ref} \tag{4}$$

$$Y = \frac{(\tau / p')}{(\tau / p')_{\max}} \tag{5}$$

$$\gamma^{ref} = \frac{(\tau / p')_{\max}}{(G_0 / p_0')} \tag{6}$$

where: γ^{p} = plastic shear strain; τ = shear stress; p' = current effective mean principal stress; p_0' = initial effective mean principal stress (= 100 kPa); $(\tau/p')_{max}$ = peak stress in the plot τ/p' vs. γ^{p} ; G_0 = initial shear modulus (= 80 MPa).

The plastic shear strain increment ($d\gamma^{p}$) is evaluated by subtracting from the total shear strain increment ($d\gamma^{t}$) the elastic one ($d\gamma^{e}$):

$$d\gamma^{p} = d\gamma^{t} - d\gamma^{e} \tag{7}$$

The elastic component ($d\gamma^{e}$) is calculated by Eqs. (8) and (9), as formulated in the recently developed quasi-elastic constitutive model (IIS model) proposed by HongNam and Koseki (2005):

$$d\gamma^{e} = d\tau / G \tag{8}$$

$$G = \frac{f(e)}{f(e_0)} \frac{G_0}{\sigma'^{n}_{0}} (\sigma_z' \sigma_r')^{n/2} \tag{9}$$

where: G = shear modulus; $f(e)=(2.17-e)^2/(1+e)$, (Hardin and Richart, 1963); $f(e_0)$ = initial void ratio function at $\sigma_z' = \sigma_r' = \sigma_\theta' = 100$ kPa; G_0 = initial shear modulus (= 80 MPa); σ'_0 = reference isotropic shear stress (= 100 kPa); σ_z' and σ_r' = vertical and radial effective stress, respectively; and n = material parameter (= 0.508).

In the laboratory tests, both drained and undrained torsional shear loadings were applied while keeping the specimen height constant (i.e., simple shear conditions). In particular, a specific amount of initial static shear was achieved by applying monotonic drained torsional shear loading; subsequently, the cyclic behavior of sand with static shear was studied under undrained condition.

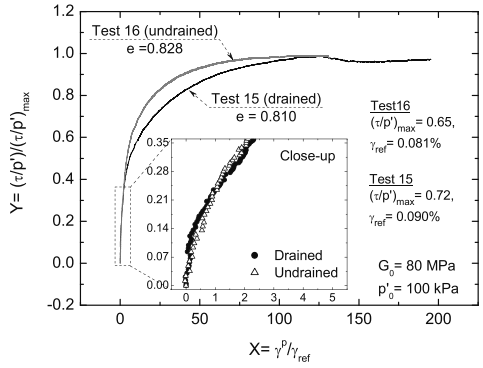

Figure 2 Comparison of X-Y relationships for drained and undrained tests.

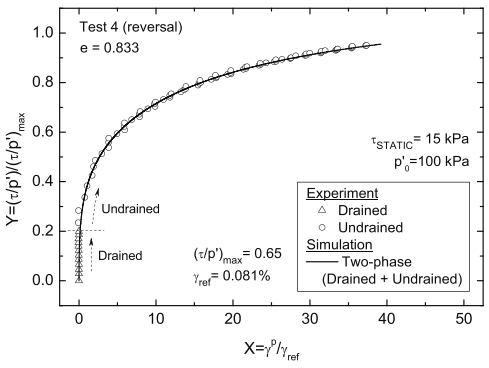

Figure 3 Typical simulation results of a two-phase skeleton curve.

Table 1 GHE parameters obtained from undrained monotonic shear tests on loose Toyoura sand Specimen (e = 0.828).

$C_1(0)$	$C_1(\infty)$	$C_2(0)$	$C_2(\infty)$	m_t	n_t	α'	β'
35	0.123	0.102	1.2	0.43	0.43	0.00501	0.92726

As shown in Fig. 2, comparison of *X-Y* relationships from drained and undrained tests revealed a similar behavior of loose sand specimens at the early stage of shearing (i.e., $Y < 0.38$). In view of this consideration and to maintain the continuity of strain development during the change of loading from drained to undrained, hereafter it is attempted to model the entire two-phase monotonic loading curve by employing a single set of GHE parameters, as listed in Table 1. Typical simulation results of two-phase skeleton curve are shown in Fig. 3.

Modeling the subsequent cyclic loading curves

It is recognized that, cyclic behavior of soil can be modeled by employing the well-known 2nd Masing's rule; however, due to rearrangement of particles, soil behavior does not necessary follow the original Masing's rule during cyclic loadings (Tatsuoka et al., 1997). This feature can be taken into account by dragging the corresponding skeleton curve in opposite direction by an amount β while applying the Masing's rule (Masuda et al., 1999; Tatsuoka et al., 2003). In this study the following drag function proposed by HongNam (2004) is used:

$$\beta = \frac{X'}{\frac{1}{D_1} + \frac{X'}{D_2}} \tag{10}$$

where: D_1 = maximum amount of drag; D_2 = fitting parameter, which is equivalent to the initial gradient of the drag function; and $X' = \Sigma \Delta X$, where ΔX denotes the increment of normalized plastic shear strain.

De Silva (2008) introduced two conceptual factors which take into account the damage (D) of plastic shear modulus at large stress level and the hardening (S) of the material during cyclic loading:

$$D = \frac{\{1 + \exp(-0.8)\}(1 - D_{ult})}{1 + \exp\left\{\left(\Sigma\left|\Delta\gamma^p\right|_p\right) - 0.8\right\}} + D_{ult} \tag{11}$$

where: D_{ult} = minimum value of D; $\Sigma|\Delta\gamma^p|_p$ = total plastic shear strain accumulated between the current and the previous turning points;

$$S = 1 + \frac{\left(\Sigma|\Delta X|\right)_{up\ to\ current\ turning\ point}}{\frac{D_2}{D_1} + \frac{\left(\Sigma|\Delta X|\right)_{up\ to\ current\ turning\ point}}{S_{ult} - 1}} \tag{12}$$

where: S_{ult} = maximum value of S after applying an infinite number of cycles; D_1 and D_2 are the same parameters used in the drag function.

After introducing drag, damage and hardening effects, the skeleton curve during cyclic loading can be modeled as follows:

$$Y = \frac{(X - \beta)}{\frac{1}{C_1(X - \beta) \times D} + \frac{|X - \beta|}{C_2(X - \beta) \times S}} \tag{13}$$

Drag, damage and hardening parameters employed in this study for loose Toyoura sand under constant amplitude cyclic shear loading are listed in Table 2.

Table 2 Drag, damage and hardening parameters.

D_1	D_2	D_{ult}	S_{ult}
0.25	12	0.6	1.05

MODELING THE UNDRAINED CYCLIC BEHAVIOR OF SAND WITH STATIC SHEAR

Stress-dilatancy relationships

It is a known fact that, volume change in drained shear loading well corresponds to the mirror image of pore water pressure build-up during undrained shear loading. Therefore, volume change is one of the key parameters that affect the behavior of sand under cyclic loading. Change of volumetric strain in different stage of loading can be described by the stress-dilatancy relationship which relates the ratio of plastic strain increments ($-d\varepsilon^p_{vol}/d\gamma^p_{vol}$) to the stress ratio ($\tau/p'$) (Shahnazari and Towhata, 1992; among others). It should be noted that, the theoretical stress-dilatancy relations, such as the Rowe's equations (Rowe, 1962), are derived only for either triaxial ($d\varepsilon_2 = d\varepsilon_3$ or $d\varepsilon_2 = d\varepsilon_1$) or simple shear ($d\varepsilon_2 = 0$) loading conditions, therefore they are not directly applicable to the case of torsional shear loading. However, the results from cyclic torsional shear tests suggest that unique relationships between $-d\varepsilon^p_{vol}/d\gamma^p_{vol}$ and τ/p' exist either for loading ($d\gamma^p > 0$) and unloading ($d\gamma^p < 0$) conditions (Pradhan et al., 1989). De Silva (2008) suggested an empirical bi-linear stress-dilatancy relationship for cyclic torsional shear loading which is linked with the damage (D) of plastic shear modulus, as reported in Eq. (14):

$$\frac{\tau}{p'} = R_k D\left(-\frac{d\varepsilon^p{}_{vol}}{d\gamma^p}\right) \pm \frac{C}{D} \tag{14}$$

where: R_k and C are the gradient and the intercept of the linear stress-dilatancy relationship, respectively; and D is the same as the damage factor in Eq. (11).

It is also recognized that, during cyclic loadings, the effective mean stress (p') decreases with number of cycles and it can be associated with two potential mechanisms: (i) the soil is subjected to significant effects of over-consolidation until the stress state exceeds for the first time the phase transformation stress state (Ishihara et al., 1975) (i.e., the first time where the volumetric behavior changes from contractive to dilative, $dp' > 0$); and (ii) soil enters into the stage of cyclic mobility. In particular, the over-consolidation significantly alters the stress-dilatancy behavior of sand during the virgin loading and its effect evanishes with the subsequent cyclic loading. To consider the effect of over-consolidation within a certain boundary, Oka et al. (1999) put forward the following stress-dilatancy equations (after De Silva, 2008):

$$-\frac{d\varepsilon^p{}_{vol}}{d\gamma^p} = \frac{D_k}{R_k}\left(\frac{\tau}{p'} - \frac{\tau/p'}{\ln(OCR)}\right) \tag{15}$$

$$D_k = \left[\frac{\tau/p'}{C\ln(OCR)}\right]^{1.5} \tag{16}$$

$$OCR = p_0'/p' \tag{17}$$

In the current study, a modification of the equations proposed by Oka et al. (1999), which consists of a rotation of over-consolidation (OC) boundary surface as schematically illustrated in Fig. 4, is

made to account for the combined effects of over-consolidation and initial static shear stress on undrained cyclic torsional shear behavior of sand. To this purpose, the following stress-dilatancy equations are proposed to define an anisotropic over-consolidation boundary surface (AOC):

$$-\frac{d\varepsilon^{p}{}_{vol}}{d\gamma^{p}} = \frac{D_k}{R_k}\left(\frac{\tau}{p'} - \frac{\tau/p' - SSR}{\ln(OCR)}\right) \tag{18}$$

$$D_k = \left[\frac{\tau/p' - SSR}{C\ln(OCR)}\right]^{1.5} \tag{19}$$

$$SSR = \tau_{static}/p_0' \tag{20}$$

where τ_{static} = initial static shear stress. Note that, whenever SSR = 0 (i.e., $\tau_{static} = 0$), Eqs. (18) and (19) meet Eqs. (15) and (16), respectively.

The proposed AOC has the same features of the one presented by Oka et al. (1999) for isotropically consolidated sands, in the sense that, it defines the region within which the specimen behaves as less contractive while being affected by over-consolidation; as well, it takes into account the effects of anisotropic consolidation induced by initial static shear stress, following the same principle of the rotation of yield surface in the stress space due to anisotropic consolidation (e.g., Taiebat and Dafalias, 2010).

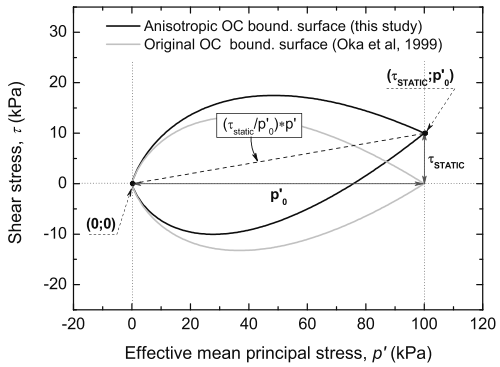

Figure 4 Schematic illustration of original (OC) and proposed (AOC) boundary surfaces.

Four-phase stress-dilatancy model

The stress path during undrained loading is divided into four sections namely: (A) Virgin stress path; (B) Stress path within the limits of phase transformation stress state; (C) Stress path within the limits of over-consolidation boundary surface; and (D) Stress path after exceeding the phase transformation stress state for the first time. The schematic illustration of the four-phase stress-dilatancy relationship is shown in Fig. 5; the coefficients and the equations employed for each phase are listed in Table 3.

Table 3 Four-phase stress-dilatancy parameters.

Phase	Eq.	R_k	C	D
A	(14)	1.7	0.595	1
B	(14)	2.2*	0.45*	1
C	(18) & (19)	2.2*	0.45*	1
D1	(14)	2.2*	0.36*	D (Eq. 11)
D2	(14)	0.33*	0.18*	D (Eq. 11)

*After De Silva (2008)

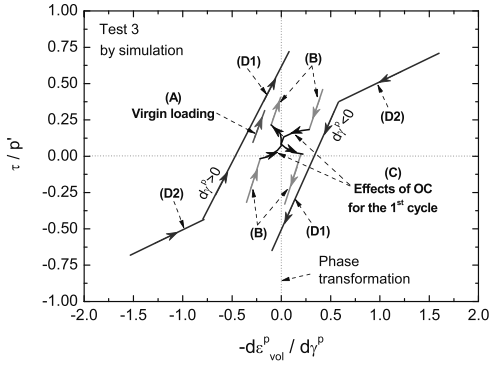

Figure 5 Typical simulation results using the four-phase stress-dilatancy relationship.

Modeling the pore water pressure generation

In modeling the undrained cyclic shear behavior it is assumed that the total volumetric strain increment ($d\varepsilon_{vol}$) during the undrained loading, which consists of dilatancy ($d\varepsilon^{d}_{vol}$) and consolidation/swelling ($d\varepsilon^{c}_{vol}$) components, is equal to zero. In fact, a change of mean effective stress (p') during undrained loading causes the re-compression/swelling of the specimen; on the other hand, a change of shear stress (τ) causes the dilatation of the specimen. Therefore the following equation is valid during undrained cyclic loading:

$$d\varepsilon_{vol} = d\varepsilon^{c}{}_{vol} + d\varepsilon^{d}{}_{vol} = 0 \tag{21}$$

Experimental evidences suggest that the bulk modulus K (= $dp'/d\varepsilon^{c}_{vol}$) can be expressed as a unique function of the effective mean principal stress (p'):

$$K = \frac{dp'}{d\varepsilon^{c}{}_{vol}} = K_0 \frac{f(e)}{f(e_o)} \left(\frac{p'}{p_0'} \right)^{m_k} \tag{22}$$

where: K_0 = bulk modulus at reference effective mean stress (p_0'); $f(e)$ and $f(e_0)$ = void ratio function at current and reference stress state, respectively; m_k = coefficient to model the stress-state dependency of K.

Considering that $f(e) = f(e_0)$ in undrained tests, and that the volumetric strain component due to consolidation/ swelling is the mirror image of the one due to dilatancy ($d\varepsilon^{c}_{vol} = -d\varepsilon^{d}_{vol}$), the generation of pore water pressure during undrained shearing was evaluated as follows:

$$dp' = K_0 \left(p' / p_0' \right)^{m_k} \left(- d\varepsilon^{d}{}_{vol} \right) \tag{23}$$

In this study, $-d\varepsilon^{d}_{vol}$ is calculated by combining the stress-strain relationship in Eq. (13) with the stress-dilatancy relations in Eq. (14) or Eq. (18). Empirically estimated value of K_0 = 47 MPa and m_k = 0.50 are used for loose Toyoura sand (e = 0.828) at an initial confining stress state of p_0' = 100 kPa.

Modeling the effect of initial static shear on the effective stress path

The presence of initial static shear widely affects the monotonic undrained behavior of sand as well as the subsequent cyclic liquefaction behavior (e.g., liquefaction resistance, failure behavior, mode of residual strain development, etc). As well, under the same initial condition of void ratio and effective mean principal stress, the peak undrained strength of sand during monotonic torsional shearing increases with the initial static shear stress (Chiaro, 2010). Herein, the presence of initial static shear stress is simulated by a monotonic drained loading path before the undrained cyclic shearing, with the

assumption that no change of p' occurs (i.e., $p' = p_0' =$ constant).

EXPERIMENTAL OBSERVATIONS AND SIMULATION RESULTS

To verify the performance of the proposed elasto-plastic model, the numerical simulation results are compared with the experimental data presented by Chiaro et al. (2011).

Typical effective stress paths obtained experimentally and by numerical simulations are shown in Figs. 6, 8 and 10. One can see that, in the case of stress-reversal loading tests, the model is able to simulate the whole liquefaction behavior of sand: specimen first enters into fully liquefied state (i.e., $p' = 0$) and then shows cyclic mobility. On the other hand, simulation results confirm that liquefaction does not take place in the case of non-reversal loading tests in a similar manner as observed in laboratory tests.

Note that, stress-reversal loading tests refers to the case in which during each cycle of loading the combined shear stress value is reversed from positive ($\tau_{max} = \tau_{static} + \tau_{cyclic} > 0$) to negative ($\tau_{min} = \tau_{static} - \tau_{cyclic} < 0$), or vice-versa; on the other hand, non-reversal loading tests refers to the case in which the combined shear stress value is always kept positive ($\tau_{min} > 0$).

Typical stress-strain relationships obtained experimentally and by numerical simulations are presented in Figs. 7, 9 and 11. The model is able to simulate qualitatively the experimental data up to a shear strain levels of about $\gamma = 8$ %, before entering a steady state (i.e., no further development of strain during subsequent cycles of loading).

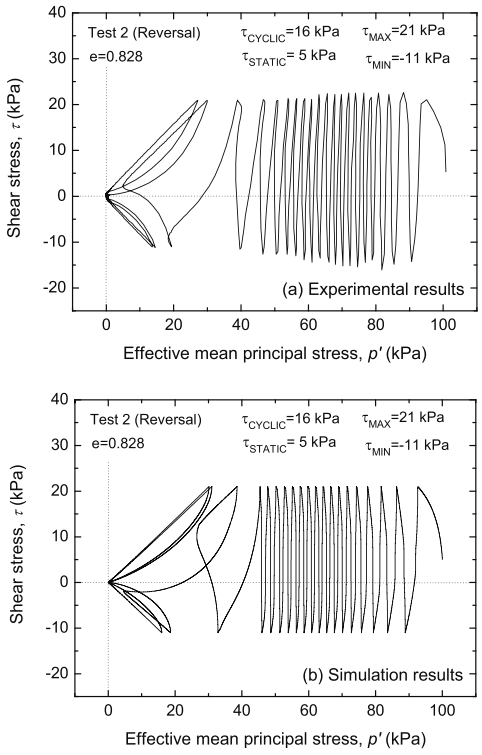

Figure 6 Effective stress paths for Tests 2

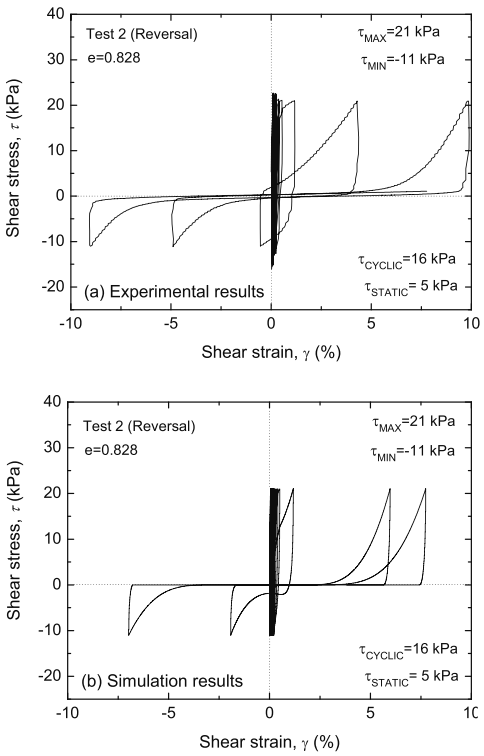

Figure 7 Stress-strain relationships for Tests 2

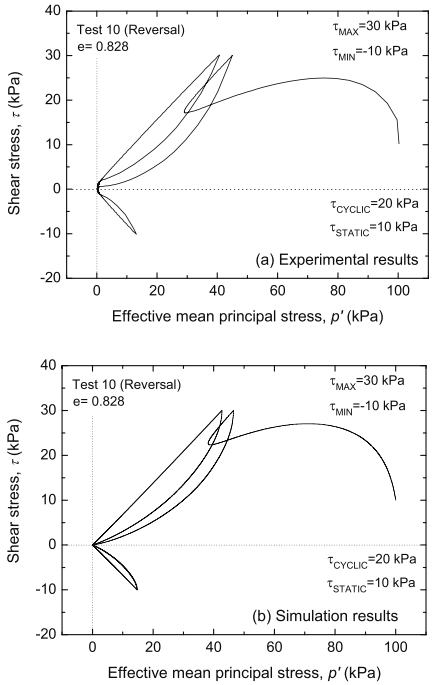

Figure 8 Effective stress paths for Test 10.

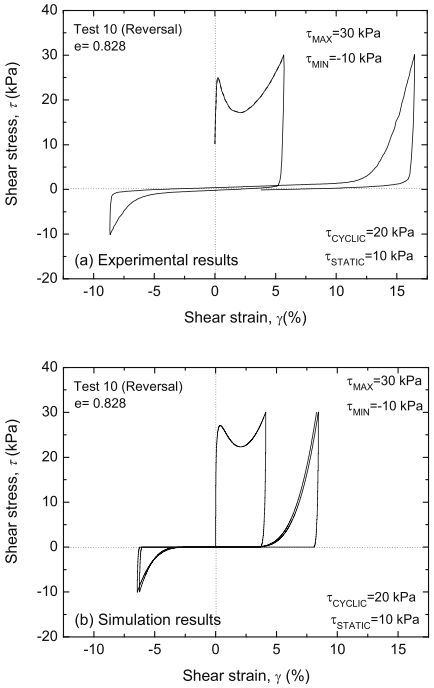

Figure 9 Stress-strain relationships for Tests 10

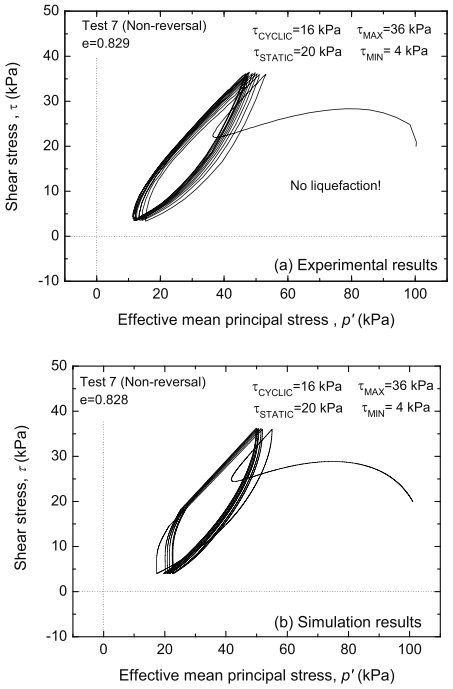

Figure 10 Effective stress paths for Test 7

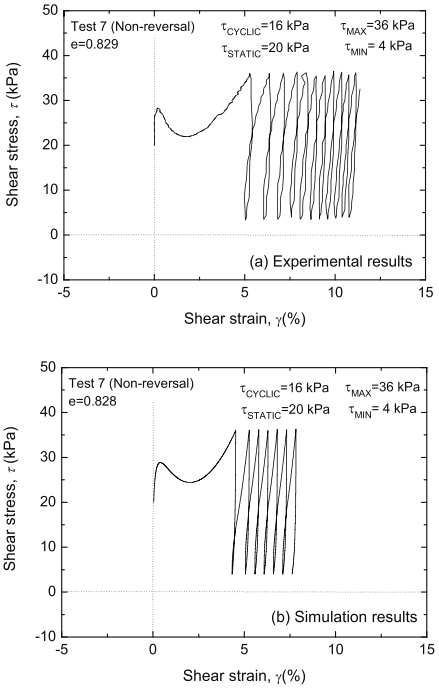

Figure 11 Stress-strain relationships for Tests 7

In this study, the resistance against liquefaction (or more strictly, resistance against cyclic shear strain accumulation) is evaluated in terms of number of cycles required to develop a specific amount of single amplitude shear strain of γ_{SA} = 7.5%, which would correspond to an axial strain ε_a = 5% in case of undrained triaxial tests.

Fig. 12 shows the comparison of experimental and simulated liquefaction resistance curves, in terms of relationships between the cyclic stress ratio CSR (= τ_{cyclic} / p_0') and the number of cycles required to develop γ_{SA} = 7.5%.

However, as suggested by Chiaro et al. (2011) the CSR is not a sufficient single parameter to describe the effects of initial static shear on the liquefaction resistance of sand; therefore, in Fig. 13, the liquefaction resistance curves are also plotted in terms of relationships between the static stress ratio SSR (= τ_{static} / p_0') and the number of cycles to develop γ_{SA} = 7.5%.

Simulation results are well consistent with the experimental data. In fact, the resistance against cyclic strain accumulation can either decrease or increase depending on the level of initial static shear and the amplitude of cyclic shear stress in a similar way as observed in laboratory tests.

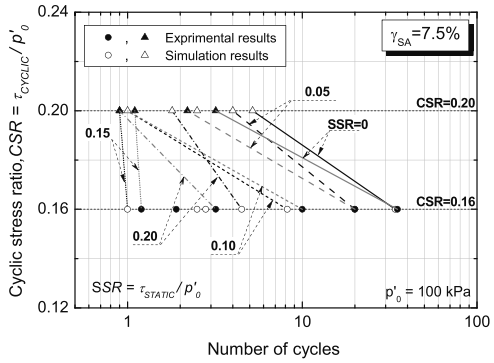

Figure 12 Liquefaction resistance curves defined in terms of cyclic stress ratio (CSR).

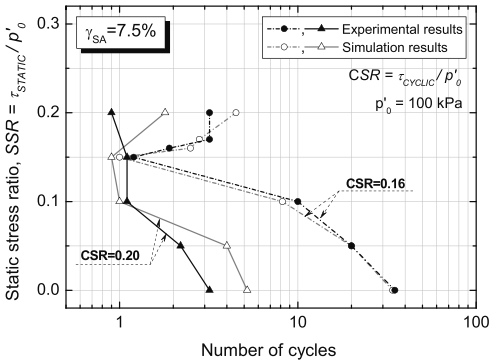

Figure 13 Liquefaction resistance curves defined in terms of static stress ratio (SSR).

EVALUATION OF FAILURE MECHANISMS FOR SAND

In Chiaro and Koseki (2010), we pointed out that failure behavior of sand with initial static shear can be associated with liquefaction (i.e., cyclic and rapid flow liquefaction behaviors) in the case of stress-reversal cyclic loadings as well as the large deformation may bring the specimen to failure (i.e., residual deformation failure behavior) in the case of non-reversal cyclic loadings. Based on these failure mechanisms and referred to undrained cyclic torsional shear behavior of sand, we proposed a practical method to assess the failure behavior of sand with initial static shear (hereafter referred as Chiaro & Koseki failure method) using as key parameters the static stress ratio (SSR), the cyclic stress ration (CSR) and the undrained strength of sand (MPSR = τ_{peak} / p_0'), where τ_{peak} is the transient monotonic undrained peak stress (Chiaro et al., 2011b).

The scheme of the proposed method is shown in Fig. 14. There are four regions that identify four failure modes, which are delineated by the following boundary conditions: (i) *{(SSR/MPSR)=(CSR/MPSR)}* characterizes the boundary between the liquefaction and no-liquefaction zones, as well as the boundary between reversal and non-reversal loading conditions; (ii) *{(SSR/MPSR)+(CSR/MPSR)=1}* defines whether the transient monotonic peak stress state is achieved or not; and (iii) test results show that in the case of reversal tests with a lower level of cyclic stress, liquefaction occurs after applying even more than a hundred cycles. Thus, considering that usually an earthquake is characterized by less than 20 cycles, under these stress conditions the probability that liquefaction takes place during an earthquake is very limited. For this reason, to take the limit of liquefaction into account, we introduced an additional boundary defining whether

liquefaction was achieved or not by applying 100 cycles of loading.

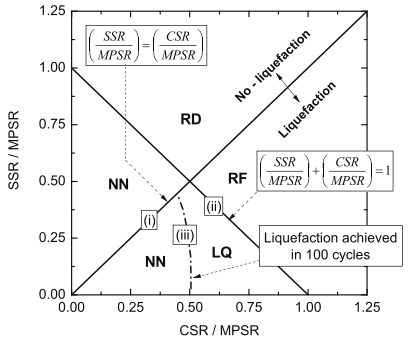

Figure 14 Failure characteristics of sand with initial static shear (after Chiaro and Koseki, 2010)
NN: no-liquefaction & no-failure; LQ: cyclic liquefaction;
RF: rapid flow liquefaction; and RD: residual deformation behavior.

Yet, the authors recognize that additional test data and/or simulation results are necessary for a better characterization of the proposed failure method for sand. Nevertheless, in performing medium size torsional shear tests, it is not easy to control accurately the initial values of density, confining pressure, static and cyclic shear stresses which are all key parameters, as well it is very time consuming; on the other hand, numerical simulations represent a good tool for validating the proposed method since all these stress parameters and density can be easily controlled. Thus, to address the analysis of failure modes of sand, using the proposed elasto-plastic model a series of numerical simulations is carried out. In order to have a less conservative approach, maximum 20 cycles of loading are applied versus 100 cycles used previously. On the contrary, the model-generated predictions are assessed by assuming that full liquefaction is achieved when the ratio between the current pore water pressure (Δu) and the initial effective mean principal stress (p_0') reaches a value of $\Delta u/p_0' = 0.98$ versus 1.00 assumed previously by Chiaro and Koseki (2010).

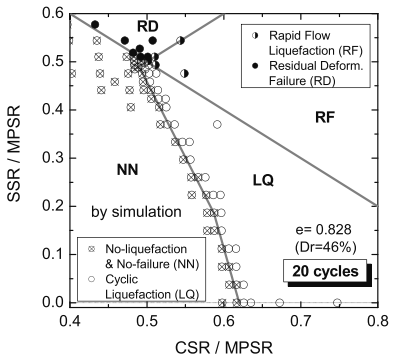

Figure 15 Boundary defining whether liquefaction ($\Delta u/p_0' = 0.98$) is achieved or not by applying 20 cycles of laoding.

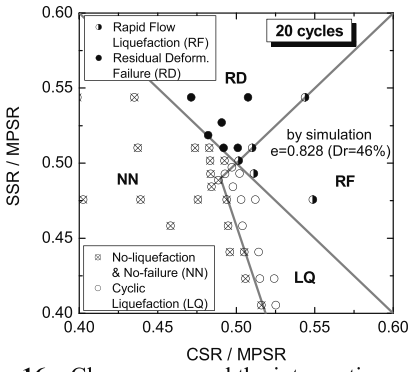

Fig. 16 Close-up around the intersection point of the four-zone failure plan

Fig. 15 shows the simulation results and the boundary defining whether liquefaction is achieved or not by applying 20 cycles of loading. On the other hand, Fig. 16 shows in details the predicted failure modes around the convergence point of the four-zone failure behaviors. This represents a critical zone due to the fact that a slight change in stress conditions brings a change in failure behavior, therefore

simulations are done for small variations of static and cyclic shear stresses (i.e., $\Delta\tau_{static}$= 0.25 kPa and $\Delta\tau_{static}$= 0.25 kPa, or even less).

The overview of the modified Chiaro & Koseki failure method for sand with initial static shear is presented in Fig. 17.

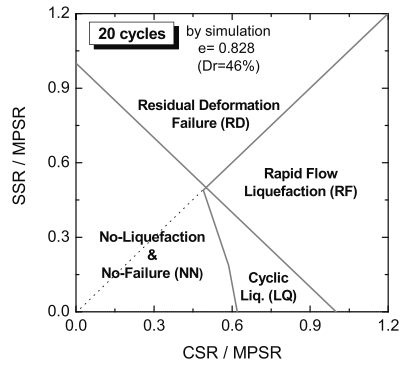

Figure 17 Modified Chiaro & Koseki failure method for sand with initial static shear.

SUMMARY AND CONCLUSIONS

In this paper, a cyclic elasto-plastic model is put forward for simulating the undrained cyclic torsional shear behavior of sand with initial static shear (i.e., sloping ground conditions).

The following characteristics are considered into the proposed model: (a) the presence of initial static shear stress is introduced by means of a monotonic drained shear loading path before the undrained one; (b) the two-phase skeleton curve (drained followed by undrained) is simulated by employing the GHE model; (c) the subsequent cyclic stress-strain behavior is modeled using the extended Masing's rules while considering the rearrangement of particles during cyclic loading, the damage of plastic shear modulus at large level of shear stress and the hardening of the material during cyclic loading; (d) the undrained cyclic shear behavior is modeled under the assumption that the total volumetric strain increment during the undrained loading is equal to zero; (e) an empirical four-phase stress-dilatancy relationship which varies with the amount of damage to the plastic shear modulus of the material is employed to model the accumulation of volumetric strain increment due to dilatancy and the generation of pore water pressure during the undrained cyclic shear loading; and (f) an anisotropic over-consolidation boundary surface is employed to account the combined effects of over-consolidation and initial static shear stress.

To verify the performance of the proposed elasto-plastic model, the simulated results are compared with the experimental data. The model has been found to be capable of reproducing all the features of the undrained cyclic torsional shear behavior of Toyoura sand specimens subjected to initial static shear stress, which are evaluated in terms of effective stress path, stress-strain relationship, liquefaction (i.e., cyclic strain accumulation) resistance curves and failure modes.

Additionally, a series of numerical simulation is carried out in order to better characterize the failure criteria proposed by Chiaro and Koseki (2010), considering maximum 20 cycles of loading and a value of $\Delta u/p_0'$= 0.98. Then, a less conservative liquefaction boundary is introduced and a modified version of the Chiaro & Koseki failure method for sand with initial static shear is presented.

REFERENCES

Chiaro, G. (2010). "Deformation properties of sand with initial static shear in undrained cyclic

torsional shear tests and their modeling", *PhD Thesis*, Dept. of Civil Eng., University of Tokyo, Japan.
Chiaro, G. and Koseki, J. (2010): "A method for assessing the failure behavior of sand with initial static shear", *Proc. of 12th International Summer Symposium*, JSCE, Funabashi, Japan, 155-158.
Chiaro, G., Sato, T., Kiyota, T. and Koseki, J. (2011a). "Effect of initial static shear stress on the undrained cyclic behavior of saturated sand by torsional shear loading", *Proc. of 5th Int. Conf. on Earthquake Geotechnical Engineering*, Santiago, Chile, CD-ROM, Paper-ID: EFFCH.
Chiaro, G., Koseki, J. and Sato, T. (2011b): "Large deformation characteristics and liquefaction properties of loose saturated Toyoura sand with initial static shear in undrained cyclic torsional shear tests", *Soils and Foundations* (to be submitted for possible publication).
De Silva, L. I. N. (2008). "Deformation characteristics of sand subjected to cyclic drained and undrained torsional loadings and their modeling", *PhD Thesis*, Dept. of Civil Eng., University of Tokyo, Japan.
Hardin, B. O. and Richart Jr., F. E. (1963). "Elastic wave velocities in granular soils", *Journal of Soil Mechanics and Foundation Division*, ASCE, 89 (SM1), 33-65.
HongNam, N. (2004): "Locally measured deformation properties of Toyoura sand in cyclic and torsional loadings and their modeling", *PhD Thesis*, Dept. of Civil Eng., University of Tokyo, Japan.
HongNam, N. and Koseki, J. (2005). "Quasi-elastic deformation properties of Toyoura sand in cyclic triaxial and torsional loadings", *Soils and Foundations*, 45 (5), 19-38.
Ishihara, K., Tatsuoka, F., and Yasuda, S. (1975). "Undrained deformation and liquefaction of sand under cyclic stresses", *Soils and Foundations*, 15 (1), 29-44.
Masuda, T., Tatsuoka, F., Yamada, S. and Sato. T. (1999). "Stress-strain behavior of sand in plane strain compression, extension and cyclic loading tests", *Soils and Foundations*, 39 (5), 31-45.
Oka, F., Yashima, A., Tateishi, Y., Taguchi, Y. and Yamashita, S. (1999). "A cyclic elasto-plastic constitutive model for sand considering a plastic-strain dependence of the shear modulus", *Geotechnique*, 49 (5), 661-680.
Pradhan, T. B. S., Tatsuoka, F. and Sato, Y. (1989). "Experimental stress-dilatancy relations of sand subjected to cyclic loading, *Soils and Foundations*, 29 (1), 45-64.
Rowe, P. W. (1962). "The stress-dilatancy relation for static equilibrium of an assembly of particle in contact", *Proc. Roy. Soc. London*, Series A, 269, 500-527.
Shahnazari, H. and Towhata, I. (2002). "Torsion shear tests on cyclic stress-dilatancy relationship of sand", *Soils and Foundations*, 42 (1), 105-119.
Taiebat, M. and Dafalias, Y. F. (2010). "Simple yield surface expression appropriate for soil plasticity", *International Journal of Geomechanics*, ASCE, 10 (4), 161-169.
Tatsuoka, F., Jardine, R. J., Lo Presti, D., Di Benedetto, H. and Kodata, T. (1997). "Characterizing the pre-failure deformation properties of geomaterials, Theme Lecture", *Proc. of 14th ICSMFE*, Hamburg, Germany, 4, 2129-2164.
Tatsuoka, F., Masuda, T., Siddiquee, M. S. A. and Koseki, J. (2003). "Modeling the stress-strain relations of sand in cyclic plane strain loading", *Journal of Geotechnical and Geoenvironmental Engineering*, ASCE, 129 (6), 450-467.
Tatsuoka, F. and Shibuya, S. (1992). "Deformation characteristics of soil and rocks from field and laboratory tests", Keynote Lecture, *9thAsian Regional Conf. on SMFE*, Bangkok, Thailand, 2, 101-170.